Supplementary Information

Supplementary Figures for:

Two-photon optogenetic toolbox for fast inhibition, excitation, and bistable modulation

Rohit Prakash[1], Ofer Yizhar[1], Benjamin Grewe[4,5], Charu Ramakrishnan[1], Nancy Wang[1], Inbal Goshen[1], Adam M. Packer[7], Darcy S. Peterka[7], Rafael Yuste[7], Mark J. Schnitzer[3,4,5,6], and ¶Karl Deisseroth[1, 2, 3, 6]

[1] Department of Bioengineering

[2] Department of Psychiatry and Behavioral Sciences

[3] Howard Hughes Medical Institute

[4]Department of Applied Physics

[5]Department of Biology

[6]CNC Program

Stanford University, Stanford, CA

[7]Department of Biological Sciences, Columbia University, New York, NY

¶To whom correspondence should be addressed:

Karl Deisseroth, M.D., Ph.D.

W083 Clark Center, 318 Campus Drive

Stanford, CA 94305

Phone: (650) 736-4325

deissero@stanford.edu

Nature Methods: doi:10.1038/nmeth.2215

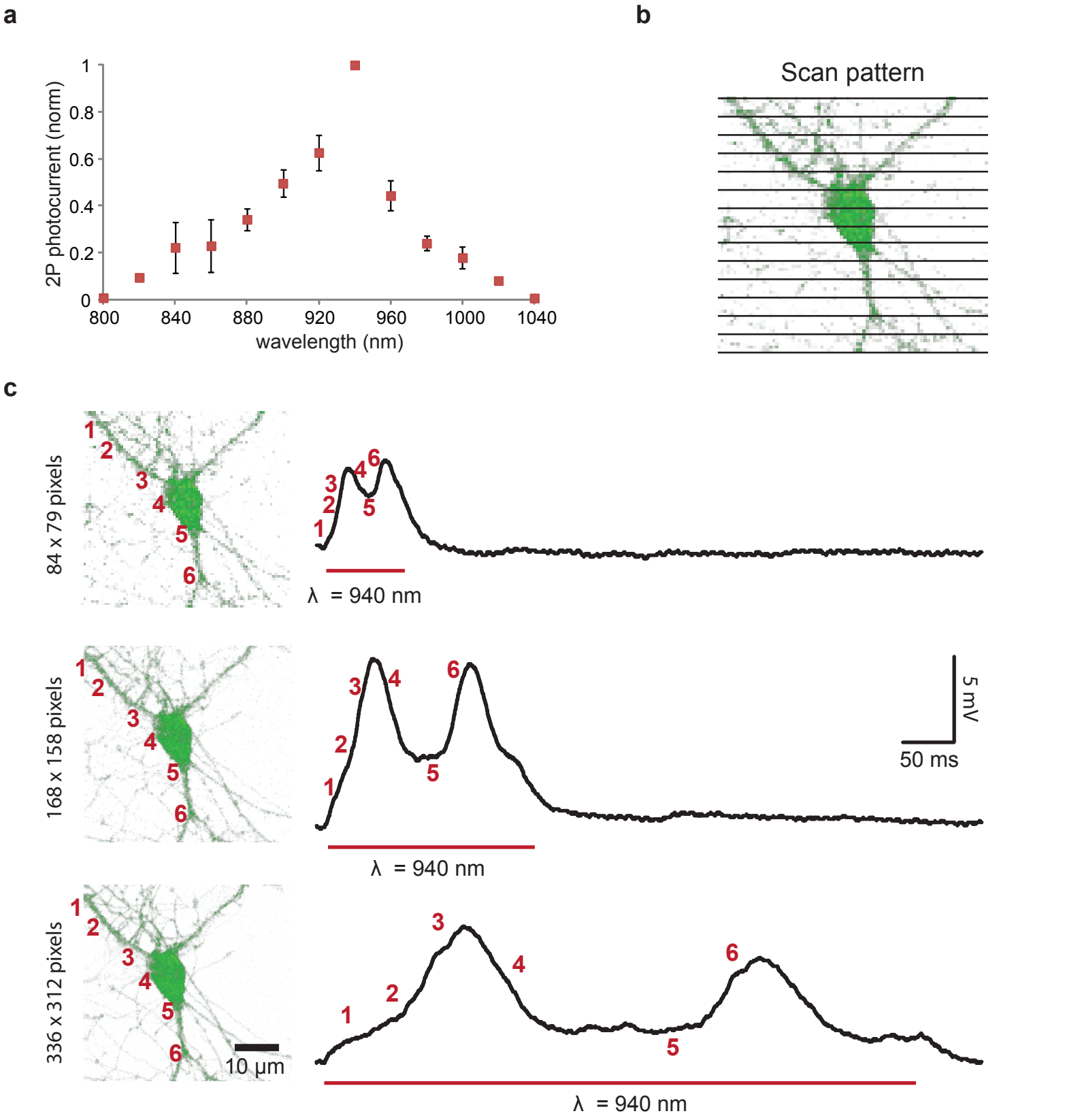
a
2P photocurrent (norm)
wavelength (nm)
b
Scan pattern
c
84 x 79 pixels
168 x 158 pixels
336 x 312 pixels
λ = 940 nm
5 mV
50 ms
10 µm

Supplementary Figure 1. Two-photon raster scanning activation of ChR2(H134R). **a.** TPLSM action spectrum of $ChR2_{HR}$-eYFP (40×/0.8NA objective; dwell time/pixel: 4.0 μs; scan resolution: 0.6 μm/pixel; line-scan speed: 0.15 μm/μs; laser intensity: 20 mW; temperature (T): 23-24°C; n = 2 cells). ROI sizes here ranged from 15x15 μm to 20x20 μm. Normalization was to the maximum photocurrent within each cell across wavelengths**. b.** Schematic of the scan pattern used below. **c.** Varying scan resolution while holding constant the dwell time/pixel at 4.0 μs; *left*, two-photon picture of stimulated hippocampal neuron in culture; *right*, current-clamp trace from the same cell. Red numbers denote both the position of the two-photon laser spot and the timepoint during the current clamp trace. Red bar: total two-photon laser time at 940 nm. This cell had a single-photon photocurrent of 1.9 nA. Other parameters were as in (**a**) (T: 23-24°C; 40×/0.8NA objective; laser intensity: 20 mW).

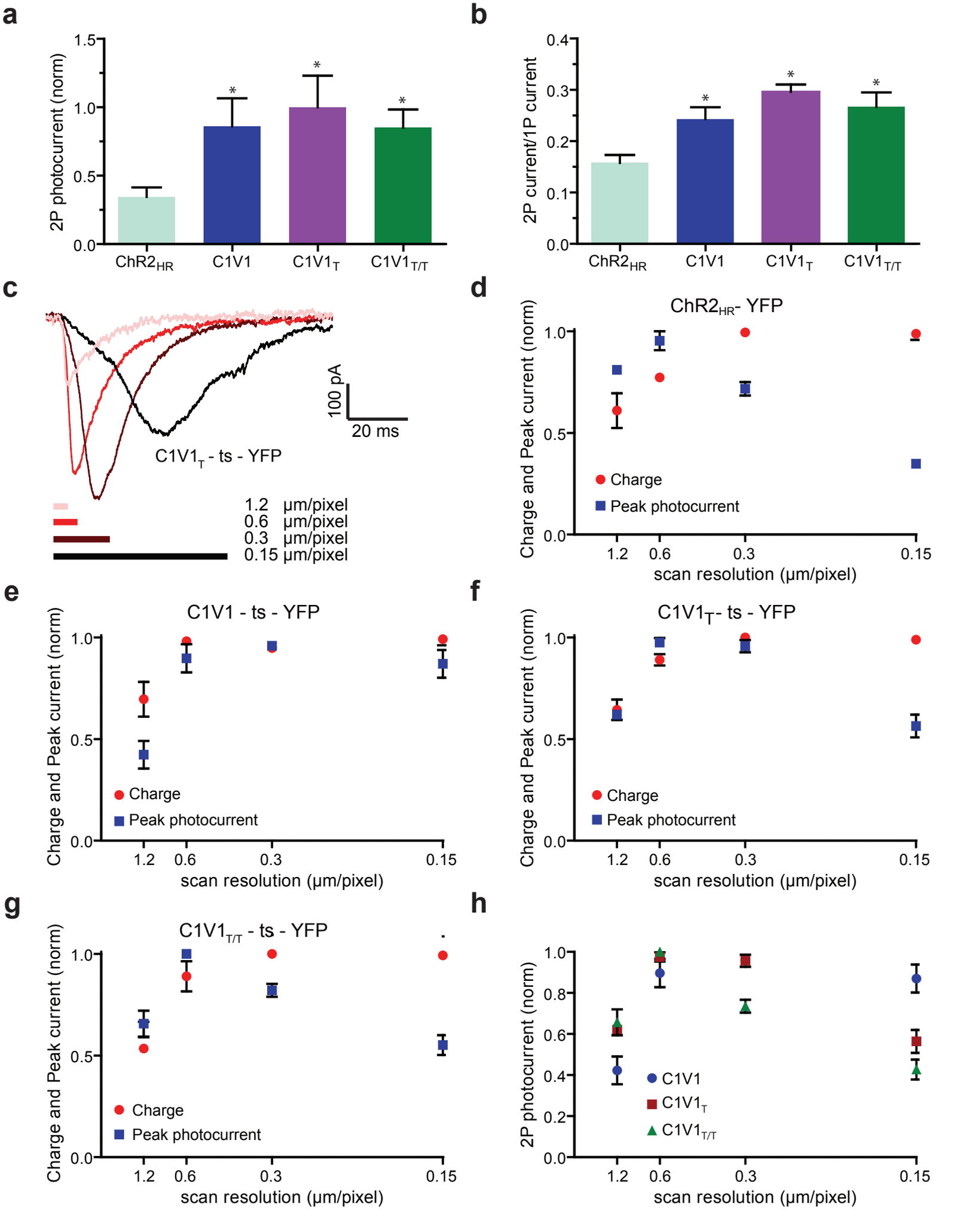
a
2P photocurrent (norm)
1.5
1.0
0.5
0.0
ChR2HR
C1V1
C1V1T
C1V1T/T
b
2P current/1P current
0.4
0.3
0.2
0.1
0.0
c
100 pA
20 ms
C1V1T - ts - YFP
1.2 µm/pixel
0.6 µm/pixel
0.3 µm/pixel
0.15 µm/pixel
d
ChR2HR- YFP
Charge and Peak current (norm)
Charge
Peak photocurrent
scan resolution (µm/pixel)
e
C1V1 - ts - YFP
f
C1V1T- ts - YFP
g
C1V1T/T - ts - YFP
h
2P photocurrent (norm)
C1V1
C1V1T
C1V1T/T

Supplementary Figure 2. Quantitative comparison and two-photon parameter mapping for C1V1 family members. a. TPLSM-elicited photocurrent comparison between $ChR2_{HR}$ and C1V1 variants [T: 23-24°C; 40×/0.8NA objective; λ= 940 nm ($ChR2_{HR}$), λ= 1040 nm (C1V1 variants); dwell time/pixel: 4.0 μs; scan resolution 0.6 μm/pixel; line scan speed: 0.15 μm/μs; laser intensity: 20 mW. ROI sizes typically ranged from 15x15 μm to 20x20 μm. Normalization is to the maximum photocurrent among all opsins (ChR2 and C1V1 variants) tested (in this case, from the $C1V1_T$ mean); error bars indicate standard error of the mean (s.e.m.); p-values were calculated allowing for a non-gaussian distribution using the Mann-Whitney two-tailed test; $ChR2_{HR}$: 0.34 ± 0.07 (n = 4 cells), C1V1: 0.86 ± 0.2 (n = 4 cells; *P=.03* vs. $ChR2_{HR}$), $C1V1_T$: 1.0 ± 0.23 (n = 4 cells; *P=.03* vs $ChR2_{HR}$), $C1V1_{T/T}$: 0.85 ± 0.13 (n = 4 cells, *P=.03* vs. $ChR2_{HR}$)]. **b.** Ratio of two-photon to single-photon photocurrents for ChR variants. Single-photon photocurrents were taken in each case by applying light power and wavelength corresponding to saturating peak photocurrent [λ= 477 nm ($ChR2_{HR}$), λ= 540 nm (C1V1 variants), light power density: 15 mW/mm^2]. Two-photon photocurrent parameters were as follows [T: 23-24°C; 40×/0.8NA objective; λ= 940 nm ($ChR2_{HR}$), λ= 1040 nm (C1V1 variants); dwell time/pixel: 4.0 μs; scan resolution: 1.2 μm/pixel; line scan speed: 0.30 μm/μs; laser intensity: 20 mW. Despite this normalization for expression level and likely off-peak two-photon excitation for C1V1 variants, C1V1 family currents remained superior; two-photon/single-photon photocurrent ratios were as follows [$ChR2_{HR}$: 0.15 ± 0.02 (n = 4 cells), C1V1: 0.24 ± 0.02 (n = 4 cells; $p<0.05$ vs. $ChR2_{HR}$), $C1V1_T$: 0.29 ± 0.01 (n = 4 cells; $p<0.05$ vs. $ChR2_{HR}$), $C1V1_{T/T}$: 0.27 ± 0.03 (n = 4 cells; $p<0.05$ vs. $ChR2_{HR}$)]. Error bars indicate SEM; p-values were calculated allowing for non-gaussian distributions using the Mann-Whitney two-tailed test. This finding may result from the fact that these typical scan times needed for mammalian neural circuitry are fast relative to opsin off-kinetics. **c.** Example voltage-clamp measurement of $C1V1_T$-ts-eYFP photocurrents with different scan resolutions (T: 23-24°C; 40×/0.8NA objective; λ= 1040 nm; dwell time/pixel: 4.0 μs; laser intensity: 20 mW). Scan resolution is represented by commonly-employed microns/pixel specifications (1.20 μm/pixel, 0.6 μm/pixel, 0.3 μm/pixel, and 0.15 μm/pixel). Bars indicate actual scan time for each condition. ROI sizes here ranged from 15x15 μm to

20x20 μm. **d.** Plot of total charge [area under the curve (AUC) of photocurrent versus time] and peak photocurrent for a given scan resolution for $ChR2_{HR}$ (T: 23-24°C; 40×/0.8NA objective; λ= 940 nm; dwell time/pixel: 4.0 μs; laser intensity: 20 mW; n = 4 cells). Normalization is to the maximum total charge transfer or peak photocurrent within a given cell across all scan resolutions; error bars indicate SEM. **e.** Plot of total charge [area under the curve (AUC) of photocurrent versus time measurement] and peak photocurrent for a given scan resolution for C1V1 (T: 23-24°C; 40×/0.8NA objective; λ= 1040 nm; dwell time/pixel: 4.0 μs; laser intensity: 20 mW; n = 4 cells). ROI sizes ranged from 15x15 μm to 20x20 μm. Normalization is to the maximum total charge transfer or peak photocurrent within a given cell across all scan resolutions; error bars indicate SEM. **f.** Plot of total charge [area under the curve (AUC) of photocurrent versus time measurement] and peak photocurrent for a given scan resolution for $C1V1_T$ (T: 23-24°C; 40×/0.8NA objective; λ= 1040 nm; dwell time/pixel: 4.0 μs; laser intensity: 20 mW; n = 4 cells). ROI sizes ranged from 15x15μm to 20x20μm. Normalization is to the maximum total charge transfer or peak photocurrent within a given cell across all scan resolutions; error bars indicate SEM. **g.** Plot of total charge [area under the curve (AUC) of photocurrent versus time measurement] and peak photocurrent for a given scan resolution for $C1V1_{TT}$ (T: 23-24°C; 40×/0.8NA objective; λ= 1040 nm; dwell time/pixel: 4.0 μs; laser intensity: 20 mW; n = 4 cells). ROI sizes ranged from 15x15 μm to 20x20 μm. Normalization is to the maximum total charge transfer or peak photocurrent within a given cell across all scan resolutions; error bars indicate SEM. **h.** Summary graph for an independent side-by-side comparison: scan resolution for C1V1 variants [C1V1: n = 5; $C1V1_T$ n = 5, $p<0.01$ vs C1V1; $C1V1_{T/T}$ n = 3, $p<0.01$ vs C1V1].

Nature Methods: doi:10.1038/nmeth.2215

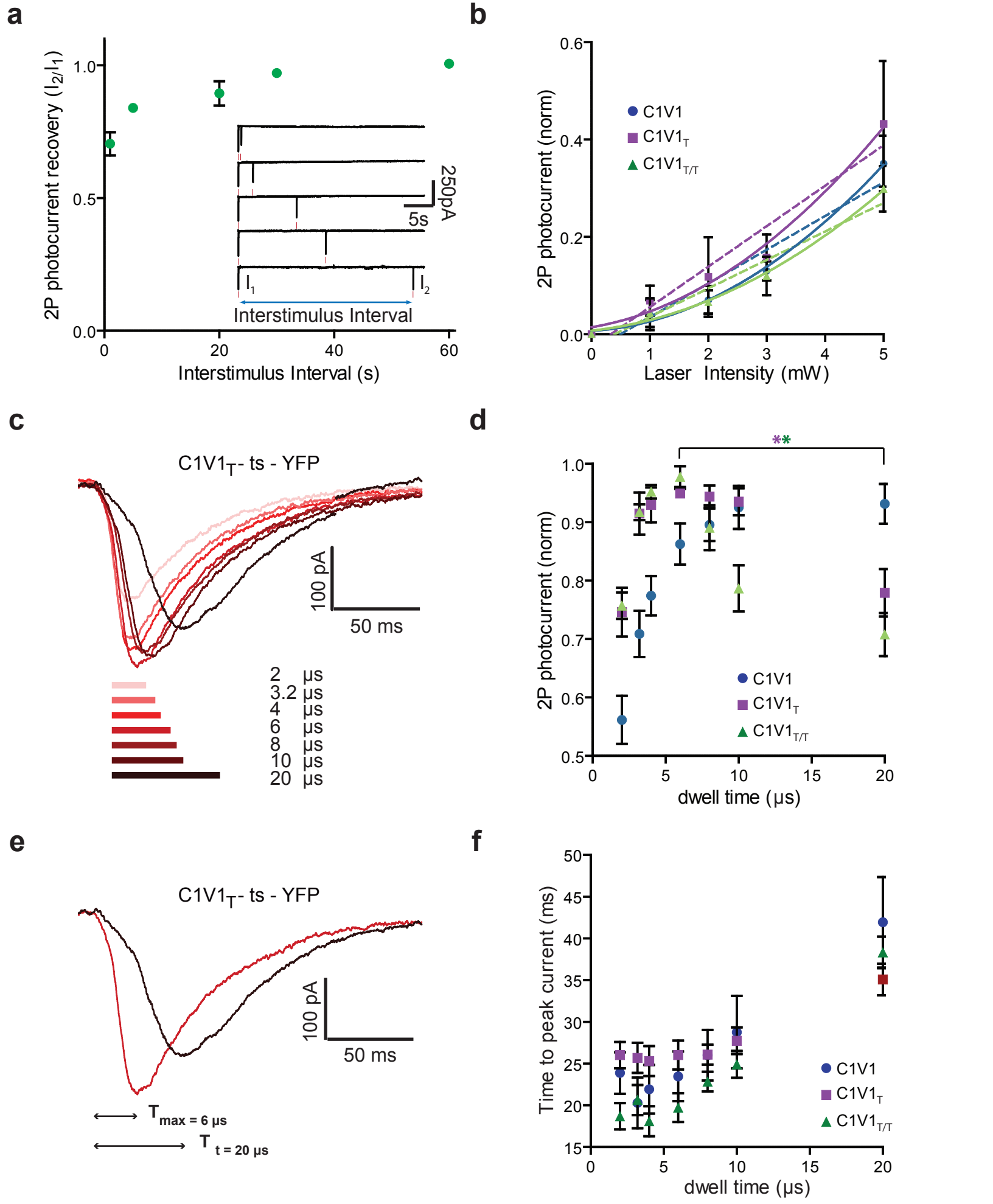
a
2P photocurrent recovery (I_2/I_1)
1.0
0.5
0.0
0
20
40
60
Interstimulus Interval (s)
250pA
5s
I_1
I_2
Interstimulus Interval
b
2P photocurrent (norm)
0.6
0.4
0.2
0.0
C1V1
$C1V1_T$
$C1V1_{T/T}$
0
1
2
3
4
5
Laser Intensity (mW)
c
$C1V1_T$- ts - YFP
100 pA
50 ms
2 µs
3.2 µs
4 µs
6 µs
8 µs
10 µs
20 µs
d
**
2P photocurrent (norm)
1.0
0.9
0.8
0.7
0.6
0.5
C1V1
$C1V1_T$
$C1V1_{T/T}$
0
5
10
15
20
dwell time (µs)
e
$C1V1_T$- ts - YFP
100 pA
50 ms
T_{max} = 6 µs
T_{t} = 20 µs
f
Time to peak current (ms)
50
45
40
35
30
25
20
15
C1V1
$C1V1_T$
$C1V1_{T/T}$
0
5
10
15
20
dwell time (µs)

Supplementary Figure 3. Impact of scanning parameters across C1V1 family variants. a. Summary plot of photocurrent recovery (ratio of responses elicited by second (I_2) and first (I_1) two-photon stimuli) as a function of inter-stimulus interval (n = 3 cells). 60s delays were built into experiments wherein multiple parameters were tested for the same cell. *Inset*, representative voltage-clamp traces from pyramidal cells in prefrontal cortex expressing C1V1$_T$-p2A-eYFP displaying recovery from desensitization (T: 32°C; 20×/0.5NA objective; λ: 1040nm; dwell time/pixel: 3.2 μs: 0.6 μm/pixel; line scan speed: 0.19 μm/μs). ROI sizes were 10x10 μm to 15x15 μm. **b.** Quadratic (solid line) versus linear (dashed line) fit for photocurrent versus laser intensity at low laser intensities indicative of the two-photon activation process [quadratic: C1V1: R^2=0.9962, C1V1$_T$: R^2=0.9842, C1V1$_{T/T}$: R^2=0.9936; linear: C1V1: R^2=0.9256, C1V1$_T$: R^2=0.9325, C1V1$_{T/T}$: R^2=0.9389; data also presented in Figure 1j]. In all cases linear fits were statistically poorer. Normalization is to the maximum photocurrent within cell across all laser intensities (highest intensities not shown to illustrate low-laser intensity properties). **c.** Example voltage-clamp trace of C1V1$_T$-ts-eYFP stimulated with different dwell times (T: 23-24°C; 40×/0.8NA objective; λ= 1040 nm; laser intensity: 20 mW). Bars indicate scan times for each condition. ROI sizes ranged from 15x15 μm to 20x20 μm. **d.** Two-photon photocurrent versus dwell time/pixel [T: 23-24°C; 40×/0.8NA objective; λ= 1040 nm; scan resolution: 0.6 μm/pixel; laser intensity: 20 mW; C1V1$_T$: 6.0μs vs. 20μs photocurrent, *P=.02*, n = 7; C1V1$_{T/T}$: 6.0μs vs. 20μs photocurrent, *P=.008*, n = 6]. ROI sizes ranged from 15x15 μm to 20x20 μm. Normalization is to the maximum photocurrent within cell across all dwell times; error bars indicate standard error of the mean (SEM). **e.** Example measurement of time to peak photocurrent. T_{max} (with a dwell time of 6 μs in this case) indicates the time it takes to reach the highest achievable (maximal) peak photocurrent within each cell across all dwell times. $T_{t=20\mu s}$ is the time to peak photocurrent for a dwell time of 20 μs, shown for comparison. **f.** Summary data relating dwell-time/pixel to time-to-peak photocurrent for each C1V1 variant. (T: 23-24°C; 40×/0.8NA objective; λ= 1040 nm; scan resolution: 0.6 μm/pixel; laser intensity: 20 mW; C1V1: n = 6; C1V1$_T$: n = 7; C1V1$_{T/T}$: n = 6). ROI sizes ranged from 15x15 μm to 20x20 μm. Normalization is to the maximum time-to-peak photocurrent within cell across all dwell times.

Nature Methods: doi:10.1038/nmeth.2215

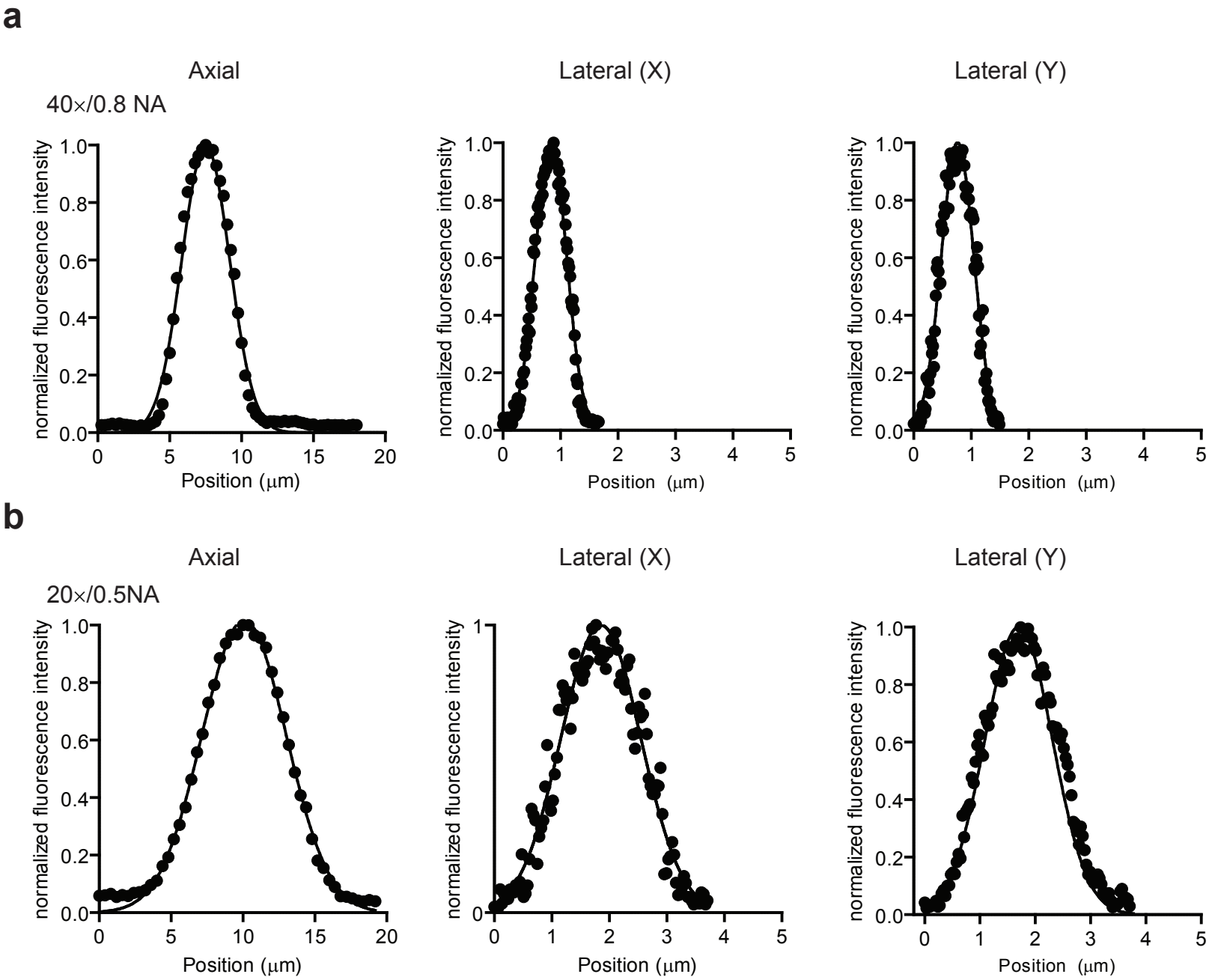

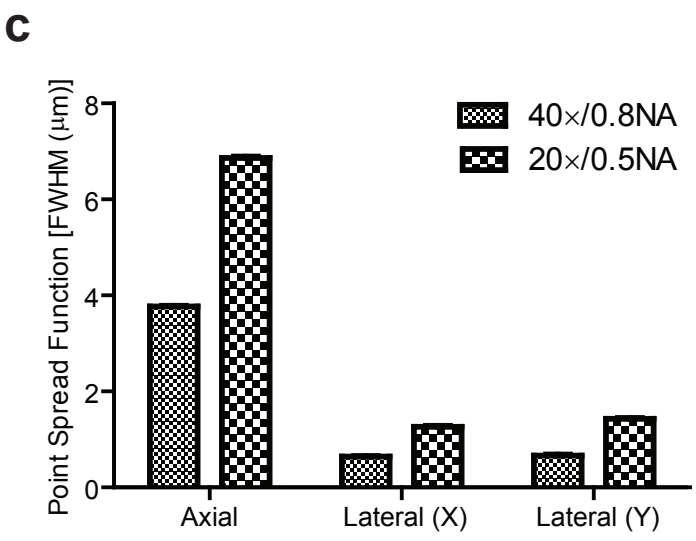

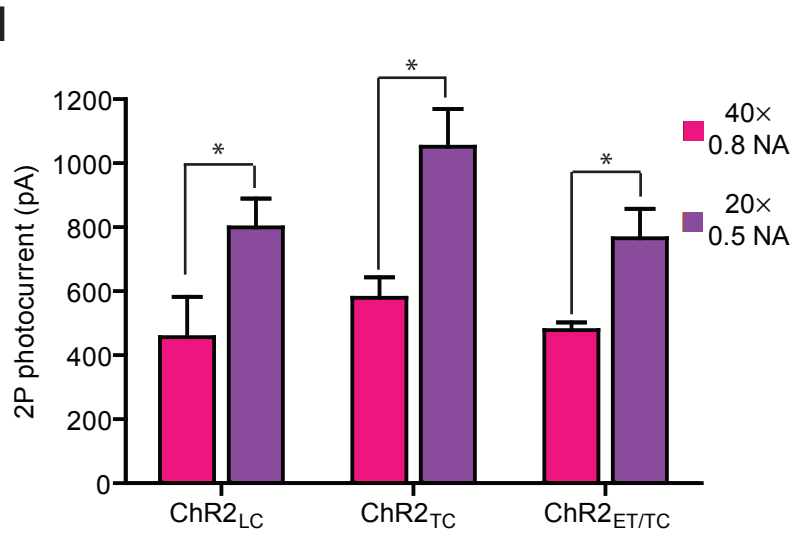

Nature Methods: doi:10.1038/nmeth.2215

Supplementary Figure 4. Objective point-spread function and quadratic two-photon properties. a. Point spread function measurements: Intensity versus position of a single 175 nm bead imaged through a 40×/0.8NA objective (λ: 1040 nm, laser intensity: 20 mW). Axial measurements represent normalized fluorescence intensity profile through the center of the bead. For the lateral plots, fluorescence intensity is measured across a single line through the center of the image at the axial plane with the maximum mean fluorescence. All plots are normalized to the maximum fluorescence. Two-photon beam profiles were measured at the back aperture of the objective; a gaussian was fit to the intensity versus position plots (in 'X' and in "Y'), and the width of the beam at $1/e^2$ intensity (the distance where intensity falls to 13.5% of the maximum value) was 7.01mm (X) and 6.7mm (Y). **b.** Point spread function measurements: Intensity versus position of a single 175 nm bead imaged through a 20×/0.5NA objective; other conditions (wavelength and laser intensity) as in A. Comparative utility assumes similar power and two-photon cross section for fluorophore and opsin. **c.** Summary full-width-half-maximum (FWHM) for the axial and lateral directions for 40×/0.8NA and 20×/0.5NA objectives [40×/0.8NA: axial = 3.77 ± 0.012 μm, n = 3 beads, lateral (X) = 0.64 ± 0.02 μm, n = 3 beads, lateral (Y) = 0.66 ± 0.017 μm, n = 3 beads; 20×/0.5NA: axial = 56.86 ± 0.054 μm, n = 3 beads, lateral (X) = 1.27 ± 0.018 μm, n = 3 beads, lateral (Y) = 1.43 ± 0.012 μm, n = 3 beads]. **d.** Two-photon photocurrents of ChR2 variants using different numerical aperture objectives [T: 23-24°C; λ: 940 nm ($ChR2_{LC}$), 960 nm ($ChR2_{TC}$) and 1000 nm ($ChR2_{ET/TC}$); laser intensity: 20 mW; for the 40×/0.8NA objective, dwell time/pixel was 4.0 μs, and scan resolution (full field of view) was 0.6 μm/pixel; for the 20×/0.5NA objective, dwell time/pixel was 4.0 μs, and scan resolution was 0.6 μm/pixel at line scan speed of 0.15 μm/μs; [$ChR2_{LC}$: 40×/0.8 photocurrent 456 ± 125 pA (n = 5 cells), 20×/0.5 photocurrent 799 ± 90 pA (n = 8 cells), *P=.05*; $ChR2_{TC}$: 40×/0.8 photocurrent 579 ± 64 pA (n = 5 cells), 20×/0.5 photocurrent 1051 ± 118 pA (n = 8 cells), *P=.006*; $ChR2_{ET/TC}$: 40×/0.8 photocurrent 478 ± 24 pA (n = 5 cells), 20×/0.5 photocurrent 765 ± 92 pA (n = 8 cells), *P=.01*]. Note that these blue-shifted variant ChRs, based on the two-photon photocurrent sizes reported here, are likely to be as (or more) potent than C1V1 family tools for two-photon control, although

in a different spectral range that may be less useful for integration with blue-shifted imaging and readout tools. ROI sizes here ranged from 15x15 μm to 20x20 μm.

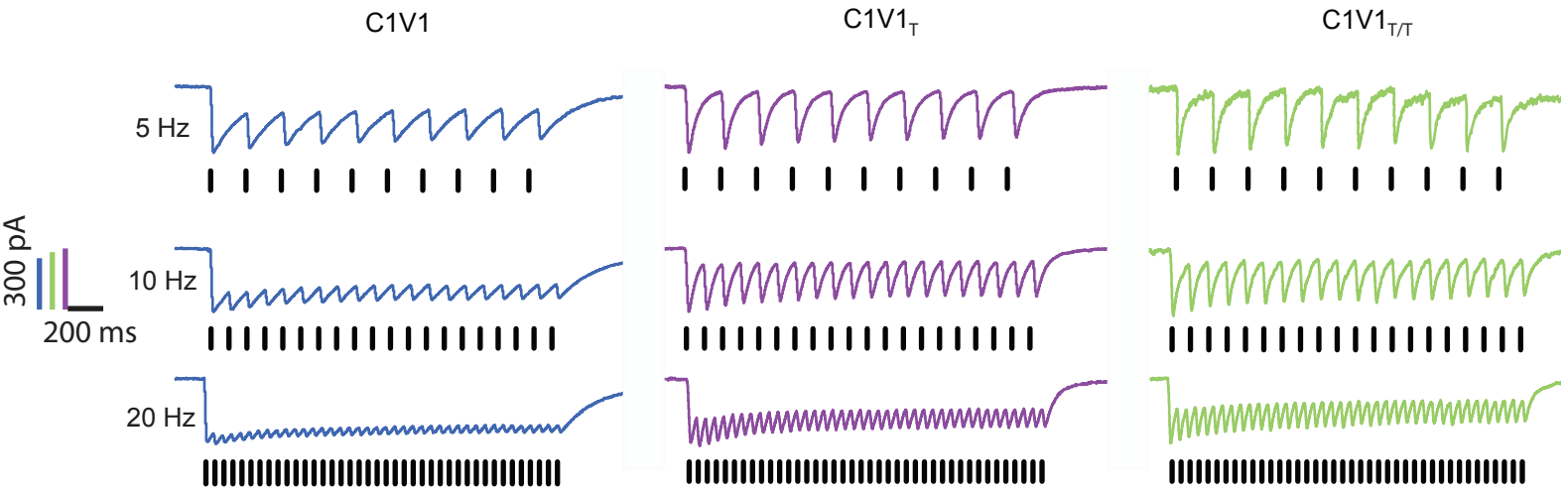

Nature Methods: doi:10.1038/nmeth.2215

Supplementary Figure 5. Differential summation of photocurrents across pulse rates for the C1V1 family. Representative voltage-clamp traces with two-photon stimulation of different C1V1 variants at 5Hz, 10Hz, and 20Hz. Black bars indicate two-photon scan timing [T: 23-24°C, 20×/.5NA objective; λ: 1040 nm; dwell time/pixel: 3.2 μs, scan resolution: 0.6 μm/pixel:; line scan speed: 0.19 μm/μs; laser intensity: 20 mW; pattern was similar for all cells tested; C1V1: n = 5; $C1V1_T$: n = 3; $C1V1_{T/T}$: n = 7]. ROI sizes here ranged from 15x15 μm to 20x20 μm.

Nature Methods: doi:10.1038/nmeth.2215

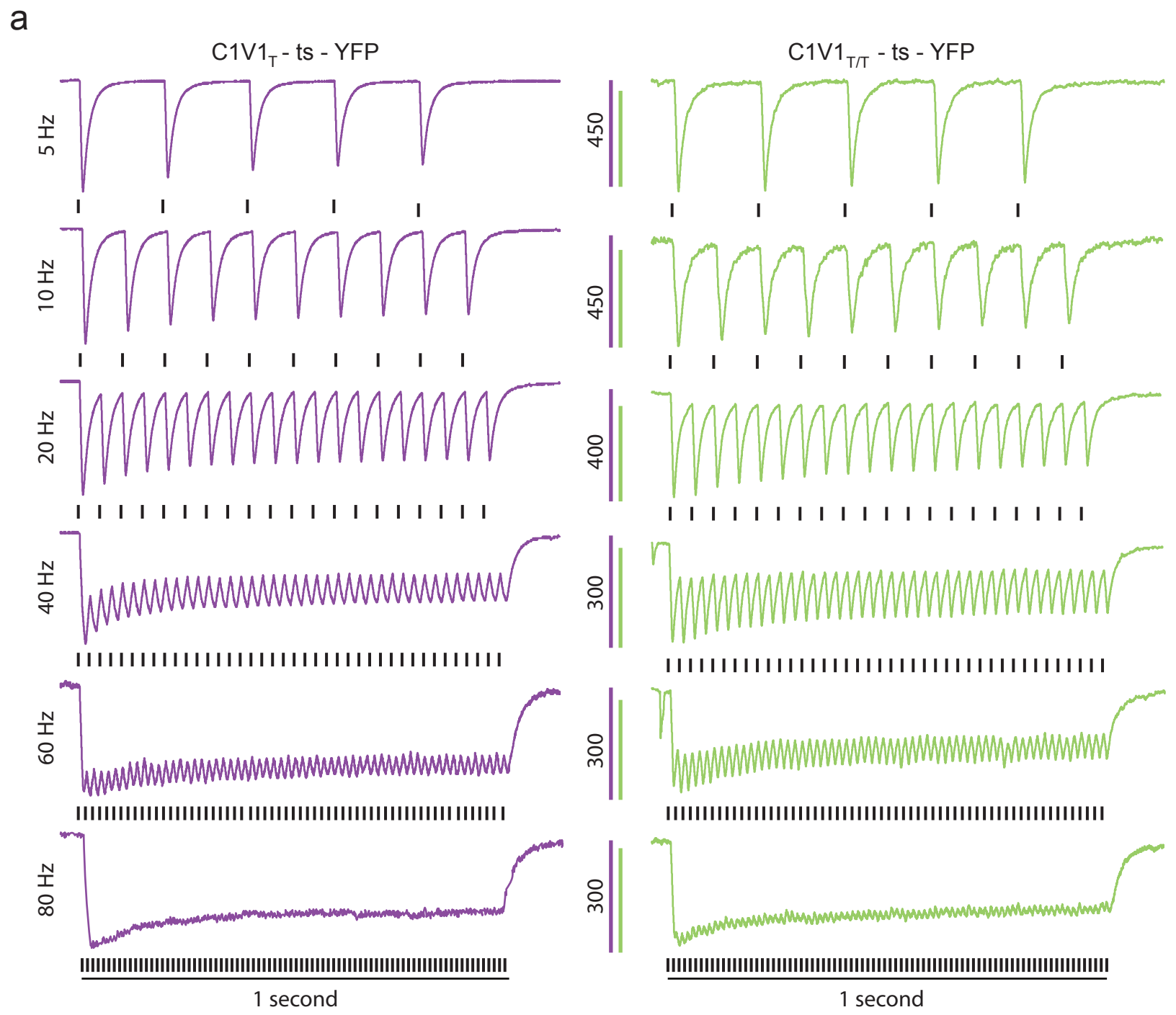
a
C1V1T - ts - YFP
C1V1T/T - ts - YFP
5 Hz
10 Hz
20 Hz
40 Hz
60 Hz
80 Hz
450
450
400
300
300
300
1 second
1 second

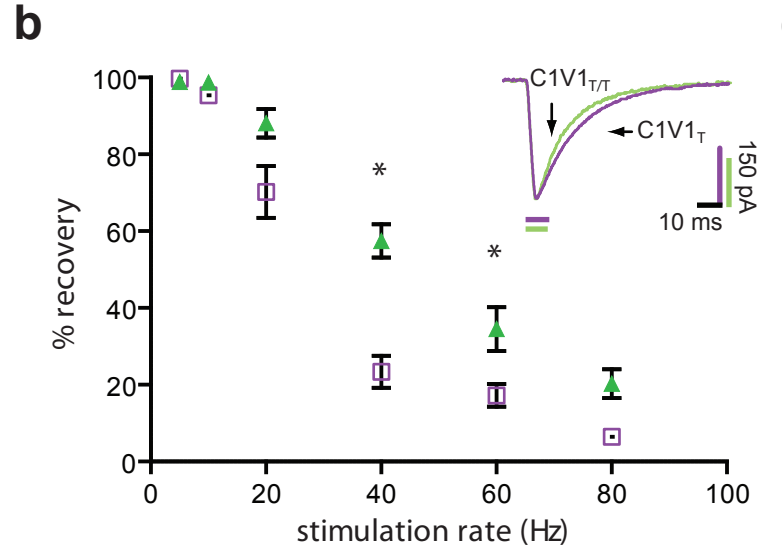
b
% recovery
stimulation rate (Hz)
C1V1T/T
C1V1T
150 pA
10 ms

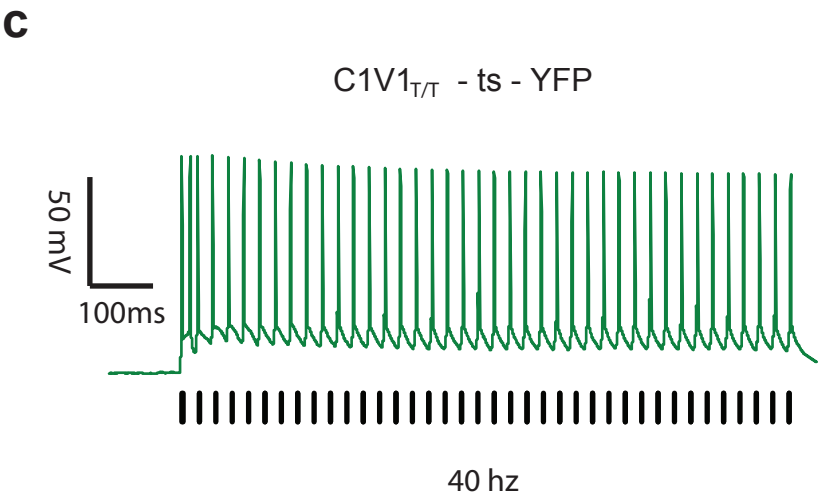
c
C1V1T/T - ts - YFP
50 mV
100ms
40 hz

Supplementary Figure 6. High-frequency performance of C1V1 variants in slice. a. Representative voltage-clamp traces in slice for $C1V1_T$ (purple) and $C1V1_{T/T}$ (green) at different stimulation frequencies (T: 32°C; 20×/.5NA objective; λ: 1040 nm; dwell time/pixel: 3.2 μs: 0.6 μm/pixel; line scan speed: 0.19 μm/μs). ROI sizes were 10x10μm to 15x15 μm. **b.** Fractional recovery of photocurrent to baseline (after the first stimulation and immediately before the second stimulation; higher recovery implies faster deactivation of the opsin after light-off) at different stimulation rates (same scan parameters as in A). $C1V1_T$ (purple): 20Hz, 70 ± 9.7% recovery, n = 5; 40Hz, 23 ± 4.2% recovery, n = 5; 60Hz, 17 ± 2.9% recovery, n = 5. $C1V1_{T/T}$ (red): 20Hz, 80 ± 2% recovery, n = 5; 40Hz, 57 ± 4.3% recovery, n = 5 (*P=.02* vs. $C1V1_T$); 60Hz, 34 ± 4.7% recovery, n = 5 (*P=.04*vs. $C1V1_T$). Error bars indicate standard error of the mean (SEM); p-values were calculated allowing for non-gaussian distributions using a Mann-Whitney two-tailed test. *Inset,* representative voltage clamp traces of two-photon activation of $C1V1_T$ (purple) and $C1V1_{T/T}$ (green) in slice. **c.** Representative current clamp trace of 1040 nm stimulation of $C1V1_{T/T}$–ts–eYFP at 40Hz; resting membrane potential –65mV; same scan parameters as in (**a**).

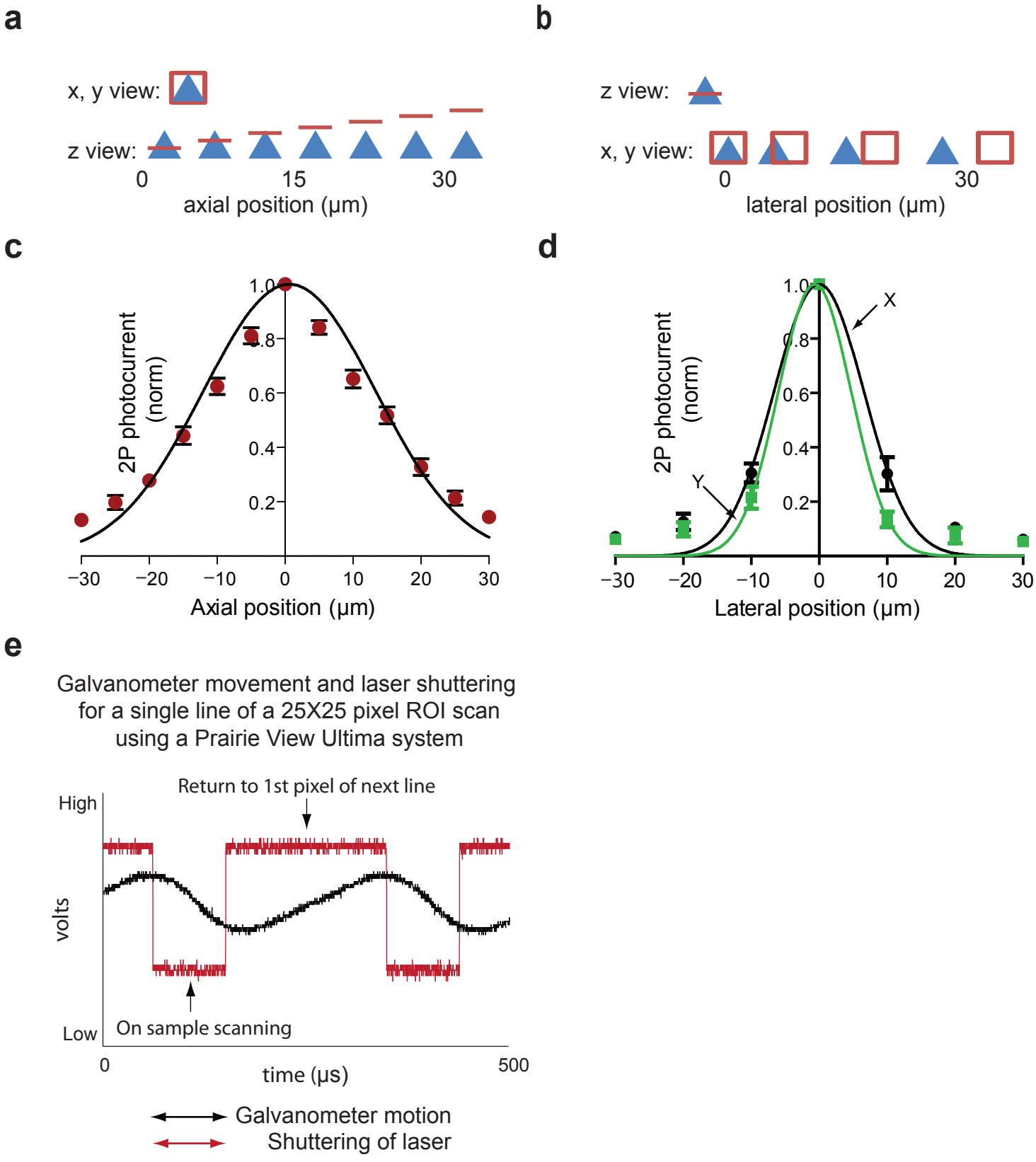
a
x, y view:
z view:
0
15
30
axial position (μm)
b
z view:
x, y view:
0
30
lateral position (μm)
c
2P photocurrent (norm)
1.0
0.8
0.6
0.4
0.2
−30
−20
−10
0
10
20
30
Axial position (μm)
d
2P photocurrent (norm)
X
Y
Lateral position (μm)
e
Galvanometer movement and laser shuttering for a single line of a 25X25 pixel ROI scan using a Prairie View Ultima system
Return to 1st pixel of next line
High
Low
volts
On sample scanning
0
500
time (μs)
Galvanometer motion
Shuttering of laser

Supplementary Figure 7. Axial and lateral resolution of two-photon C1V1 photocurrents in slice. a. Schematic of axial resolution experiment for photocurrent dependence on axial position of ROI relative to center of the cell body. Blue triangles indicate pyramidal neuron and red boxes indicate typical ROI. **b.** Schematic of corresponding lateral resolution experiments. **c.** Axial resolution of two-photon induced currents from pyramidal cells in prefrontal cortex expressing $C1V1_T$ in slice (T: 32°C; 20×/.5NA objective; λ: 1040 nm; dwell time/pixel: 3.2 μs; scan resolution: 0.6 μm/pixel; line scan speed: 0.19 μm/μs; laser intensity: 20 mW; n = 10; points fit with Gaussian, FWHM = 29.5μm; normalization is to the maximum photocurrent within cell across all axial positions; error bars indicate standard error of the mean). ROI sizes were 10x10μm to 15x15μm. **d.** Two-photon photocurrent as a function of lateral distance of ROI from the center of a pyramidal cell expressing $C1V1_T$ in slice in the 'x' (black) and 'y' (green) directions (scan parameters as in C; n = 7; normalization is to the maximum photocurrent within cell across all lateral positions). **e**. Plot of the drive signal for the x-galvanometer (black) along a single line along with "flyback" time or return to the first pixel of the next line for this unidirectional scanning mode. Also shown is the drive voltage to the pockel cell (red) corresponding to shuttering of the laser for a single line along with initiation of exposure at the first pixel of the next line of a 25x25 pixel ROI [dwell time/pixel: 3.2 μs; scan resolution (full field of view): 1024 pixels/line; line scan speed: 0.19 μm/μs]. Shuttering of the laser to open occurs at the first pixel of a line and closes at the last pixel, so that direct laser irradiation on the sample occurs in the defined ROI. Overscan is the ratio of the pockel cell *on* (red arrow, single scan) to the total galvanometer motion (black arrow, single scan), which for a typical ROI shown here is 8-9%. The total on-sample exposure time for optimized scanning conditions in culture experiments was typically 4-5ms, and for slice and in *vivo* was typically 3-4 ms; relevant calculations are described in the online methods. For the scanning parameters used here, fly-back time was typically 2-3x exposure time. For representation of stimulus timing in all figures, black tick marks are aligned to the signal controlling voltage applied to the pockel cell (via a Conoptics Modulation Box) that shutters the two-photon laser on at the very first pixel of a single line of an ROI. Likewise light-off is

defined as the place and time where the pockel cell shutters the laser to an off position after the last pixel of the final line in an ROI.

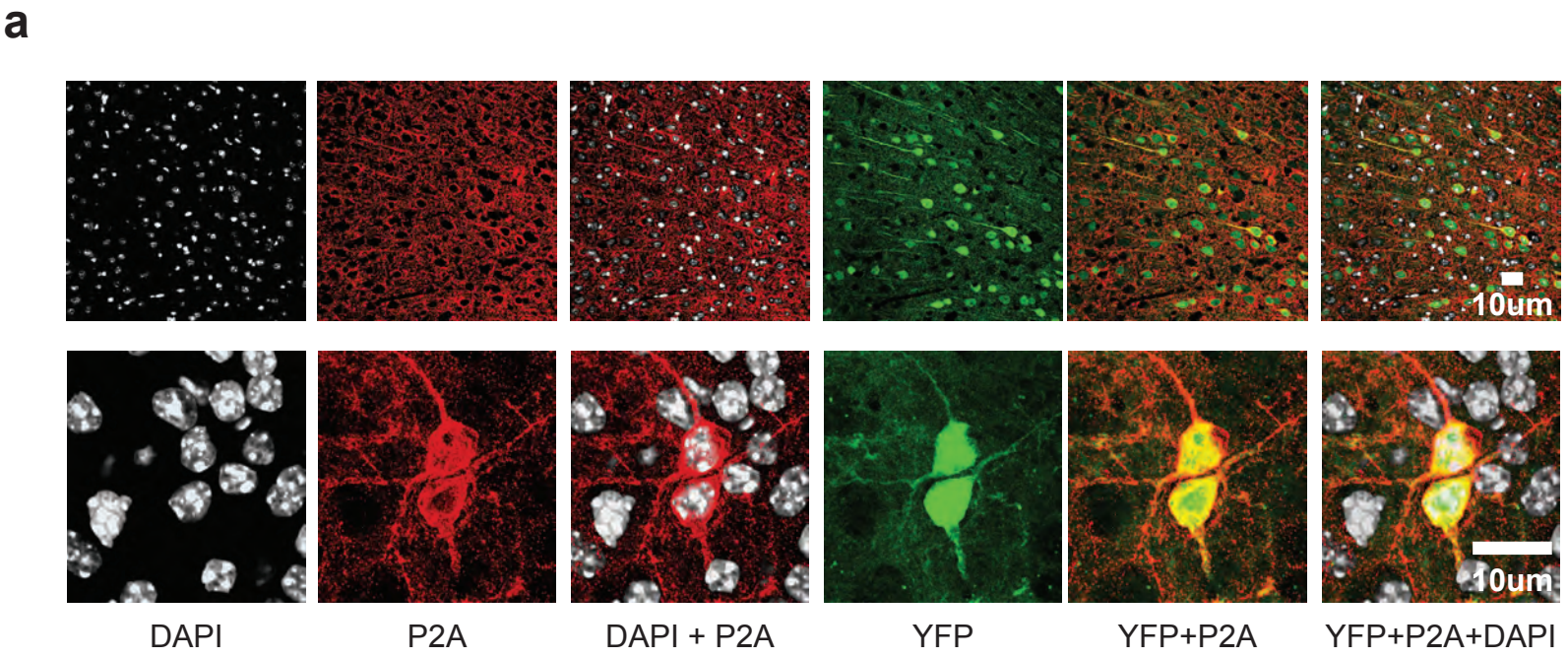

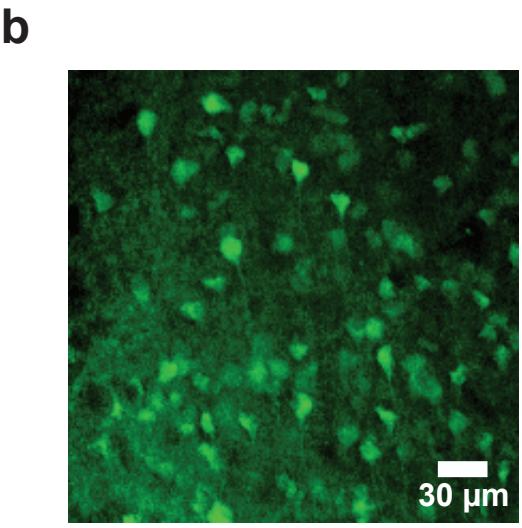

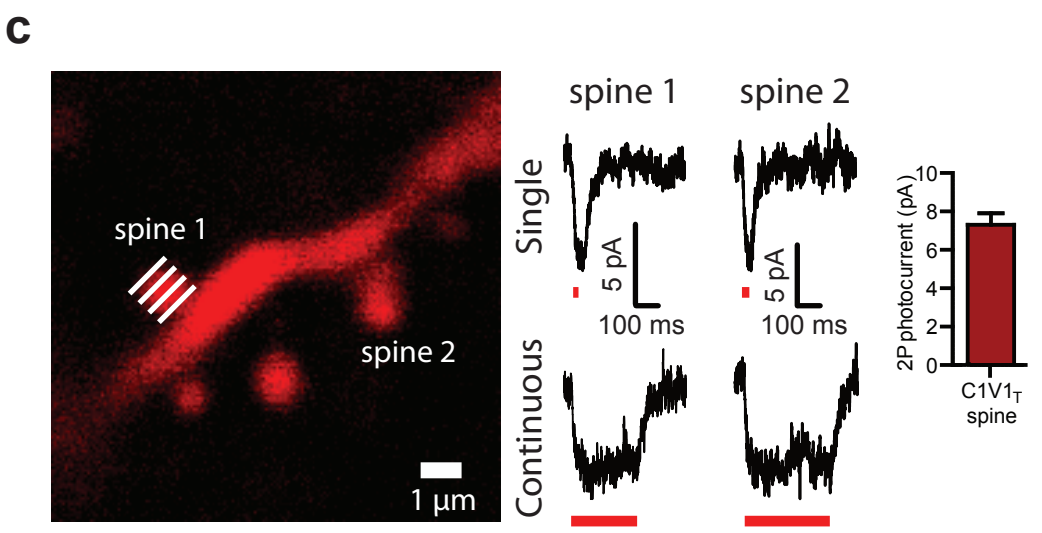

Nature Methods: doi:10.1038/nmeth.2215

Supplementary Figure 8. Versatility of the cell-filling (separated-opsin) configuration. a. *Top*, cortical neurons expressing C1V1$_T$-p2A-eYFP showing eYFP staining and location of the opsin (identified with antibody staining of the p2A motif). *Bottom*, close-up of two neurons showing opsin localization. **b.** Two-photon image (20×/0.5NA) of pyramidal cells in prefrontal cortex expressing C1V1$_T$-p2A-eYFP. **c.** (left) Two-photon picture of dendritic spines from a pyramidal cell in slice expressing C1V1$_T$-p2A-eYFP. Dendritic spines were stimulated using a 40×/0.8NA objective at 20 mW (λ: 1040 nm). White lines indicate pattern of stimulation over spine. *Right*, representative traces of two identified spines being stimulated with a single scan or continuous scans over the spine. (T: 32°C; 40×/.8NA objective; λ: 1040 nm; dwell time/pixel: 3.2 μs; scan resolution: 0.6 μm/pixel; line scan speed: 0.19 μm/μs; laser intensity: 20 mW; similar results obtained in n = 10 cells and n = 29 spines with mean photocurrent 7.3 ± 0.6 pA). Red bar indicates laser scan timing.

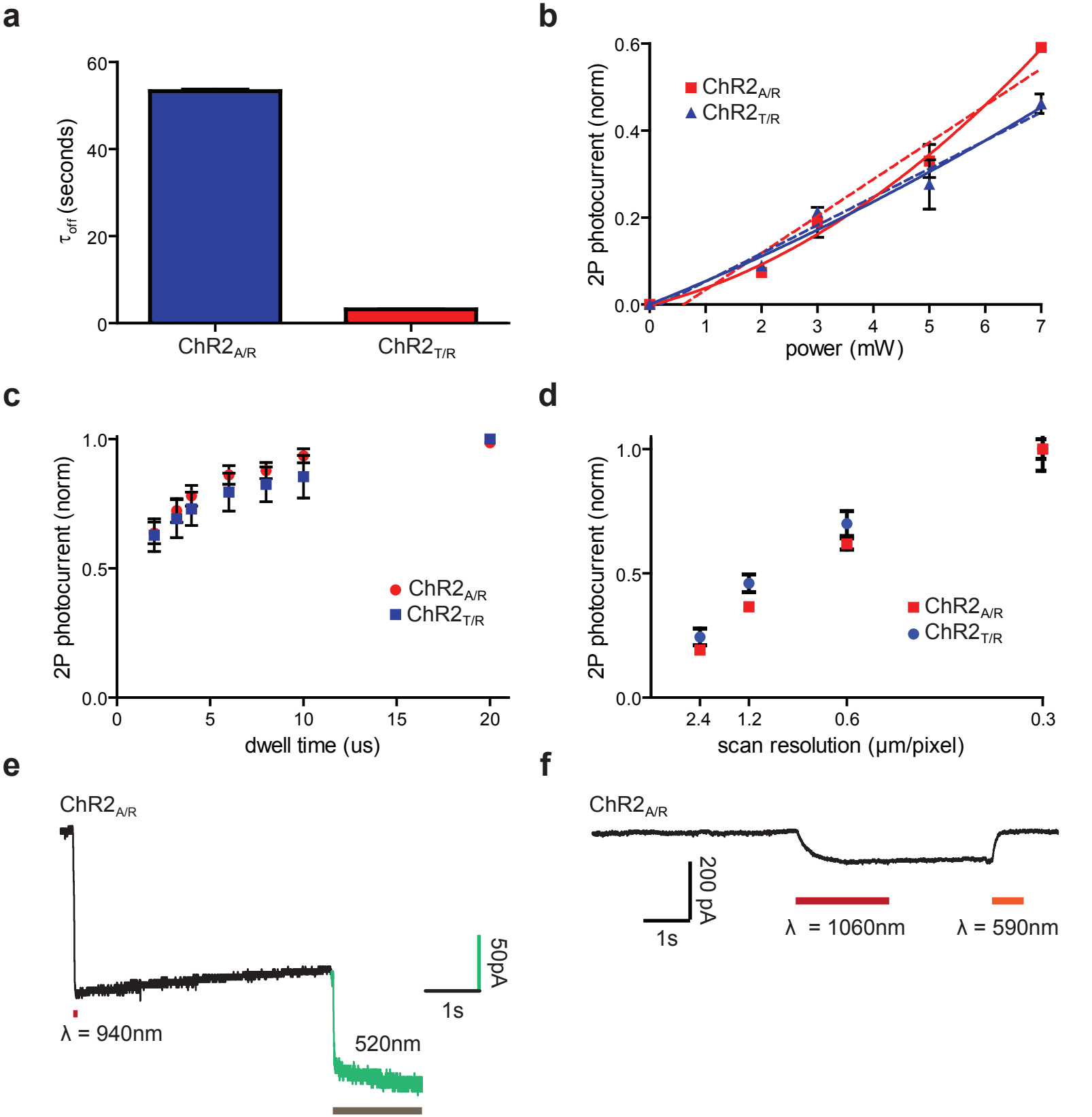

Nature Methods: doi:10.1038/nmeth.2215

Supplementary Figure 9. Spectral and kinetic parameter space mapping for bistable two-photon control tools. a. τ_{off} for 2PSFOs (T: 23-24°C; 40×/0.8NA objective; λ: 940 nm; dwell time/pixel: 4.0 μs; scan resolution: 0.6 μm/pixel; line scan speed: 0.15 μm/μs; laser intensity: 20 mW; $ChR2_{T/R}$ τ_{off} = 3.2 ± 0.05s, n = 8 cells; $ChR2_{A/R}$ τ_{off} = 53.3 ± 2.8s, n = 13 cells). ROI sizes ranged from 15x15μm to 20x20μm. **b.** Quadratic (solid line) versus linear (dashed line) fit to photocurrent versus laser intensity at low laser intensities indicative of the two-photon activation process (quadratic: $ChR2_{A/R}$ R^2=0.9940, $ChR2_{T/R}$ R^2=0.9759; $ChR2_{A/R}$ R^2=0.9589; $ChR2_{T/R}$ R^2=0.9619; data are also presented in Fig. 5F). In all cases linear fits were statistically poorer. Normalization was to the maximum photocurrent within cell across all powers. **c.** Two-photon photocurrent versus dwell time/pixel (T: 23-24°C; 40×/0.8NA objective; λ: 940 nm; scan resolution: 0.6 μm/pixel; laser intensity: 20 mW; $ChR2_{AR}$, n = 3 cells; $ChR2_{TR}$, n = 4 cells). ROI sizes ranged from 15x15μm to 20x20μm. Normalization was to the maximum photocurrent within each cell across all dwell times. **d.** Two-photon photocurrent versus scan resolution (T: 23-24°C; 40×/0.8NA objective; λ: 940 nm; dwell time/pixel: 4.0 μs; laser intensity: 20 mW; $ChR2_{AR}$, n = 7 cells; $ChR2_{TR}$, n = 6 cells). ROI sizes ranged from 15x15μm to 20x20μm. Normalization was to the maximum photocurrent within each cell across all scan resolutions. **e.** Full-field single-photon illumination can recruit 2PSFOs not recruited by a single two-photon raster scan; further single-photon activation is shown (timing shown by gray bar and green trace segment; λ: 520 nm; light power density: 5 mW/mm^2) after two-photon-activation of $ChR2_{A/R}$ photocurrents (T: 23-24°C; 40×/0.8NA objective, λ: 940 nm (red bar); other two-photon scan parameters as in A). **f.** Two-photon activation of $ChR2_{AR}$ at 1060 nm, showing that the same wavelength of light that deactivates SFOs can also activate, depending on the starting state of the opsins in the photocycle; activation and deactivation spectra overlap (T: 23-24°C; 40×/0.8NA objective; λ: 1060 nm (red bar); dwell time/pixel: 4.0 μs; scan resolution: 0.6 μm/pixel; line scan speed: 0.15 μm/μs; laser intensity: 15 mW). ROI sizes ranged from 15x15 μm to 20x20 μm. Here activation is followed by single-photon deactivation with 590 nm.

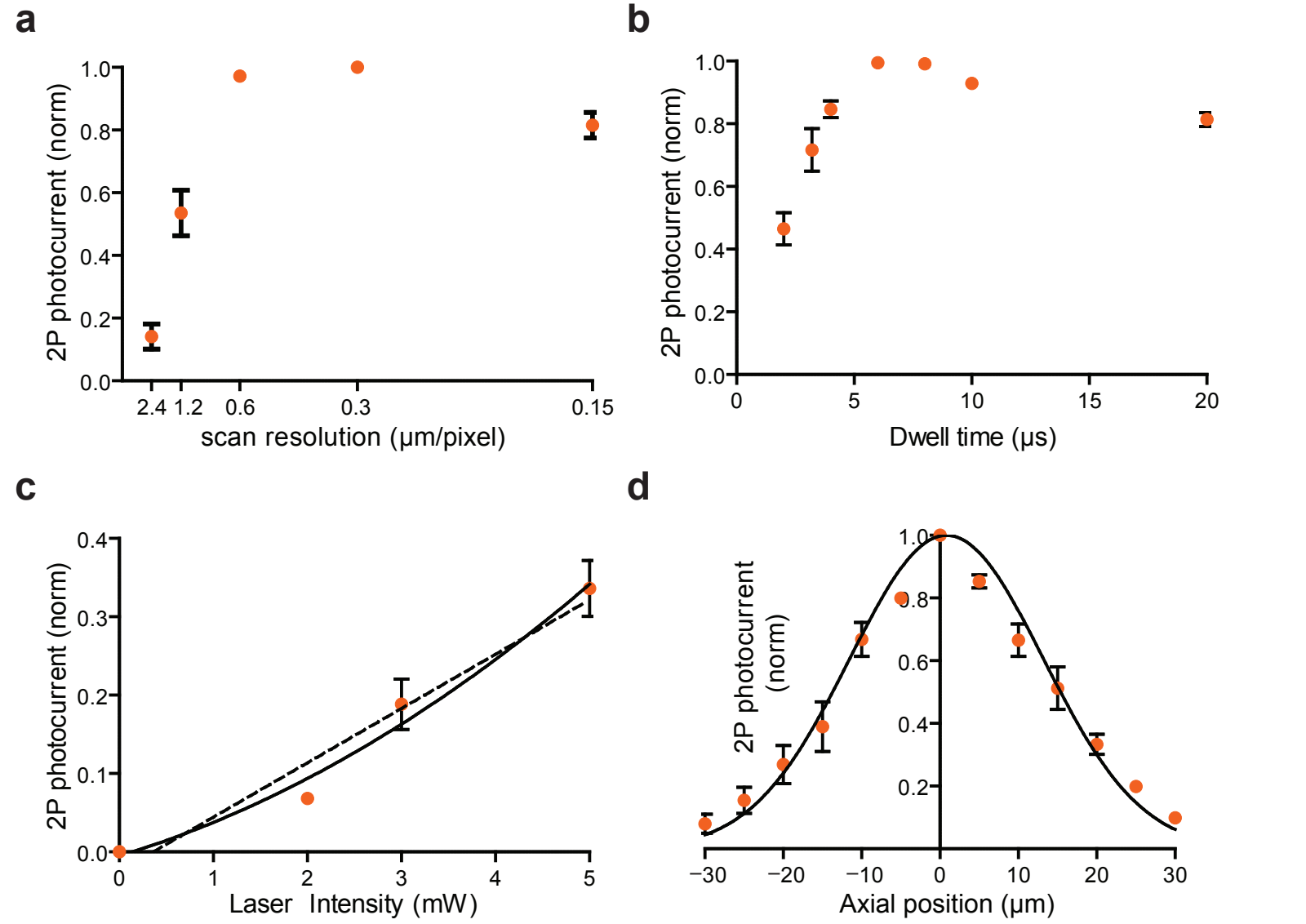
a
2P photocurrent (norm)
1.0
0.8
0.6
0.4
0.2
0.0
2.4 1.2 0.6 0.3 0.15
scan resolution (µm/pixel)
b
2P photocurrent (norm)
1.0
0.8
0.6
0.4
0.2
0.0
0 5 10 15 20
Dwell time (µs)
c
2P photocurrent (norm)
0.4
0.3
0.2
0.1
0.0
0 1 2 3 4 5
Laser Intensity (mW)
d
2P photocurrent (norm)
1.0
0.8
0.6
0.4
0.2
−30 −20 −10 0 10 20 30
Axial position (µm)

Supplementary Figure 10. Mapping parameters governing two-photon optogenetic inhibition. a. Two-photon photocurrent versus scan resolution [T: 23-24°C; 40×/0.8NA objective; λ: 1040 nm; dwell time/pixel: 4.0 μs; laser intensity: 20 mW; n = 2 cells]. ROI sizes ranged from 15x15μm to 20x20μm. Normalization was to the maximum photocurrent within each cell across all scan resolutions; error bars indicate standard error of the mean (SEM). **b.** Summary data of two-photon photocurrent versus dwell time [T: 23-24°C; 40×/0.8NA objective; λ: 1040 nm; scan resolution: 0.6 μm/pixel; laser intensity: 20 mW; n = 3 cells]. ROI sizes ranged from 15x15μm to 20x20μm. Normalization was to the maximum photocurrent within each cell across all dwell times; error bars indicate SEM. **c.** 1040 nm-evoked photocurrent versus axial position of ROI; pyramidal cells expressing eArch3.0 were stimulated within acute slice preparations from prefrontal cortex (T: 32°C; 20×/.5NA objective; λ: 1040 nm; dwell time/pixel: 4.0 μs; scan resolution: 0.6 μm/pixel line scan speed: 0.15 μm/μs; laser intensity: 20 mW; n = 4 cells; FWHM of curve shown: 28μm). ROI sizes were 10x10μm to 15x15μm. Normalization was to the maximum photocurrent within each cell across all axial positions; error bars indicate SEM. **d.** Quadratic (solid line) versus linear (dashed line) fit to photocurrent vs. laser intensity at low laser intensities indicative of the two-photon activation process (quadratic: R^2=0.9891; linear: R^2=0.9548; data are also presented in Fig. 6e). Linear fits were statistically poorer than quadratic. ROI sizes ranged from 15x15 μm to 20x20 μm. Normalization was to the maximum photocurrent within each cell across all intensities; error bars indicate SEM.

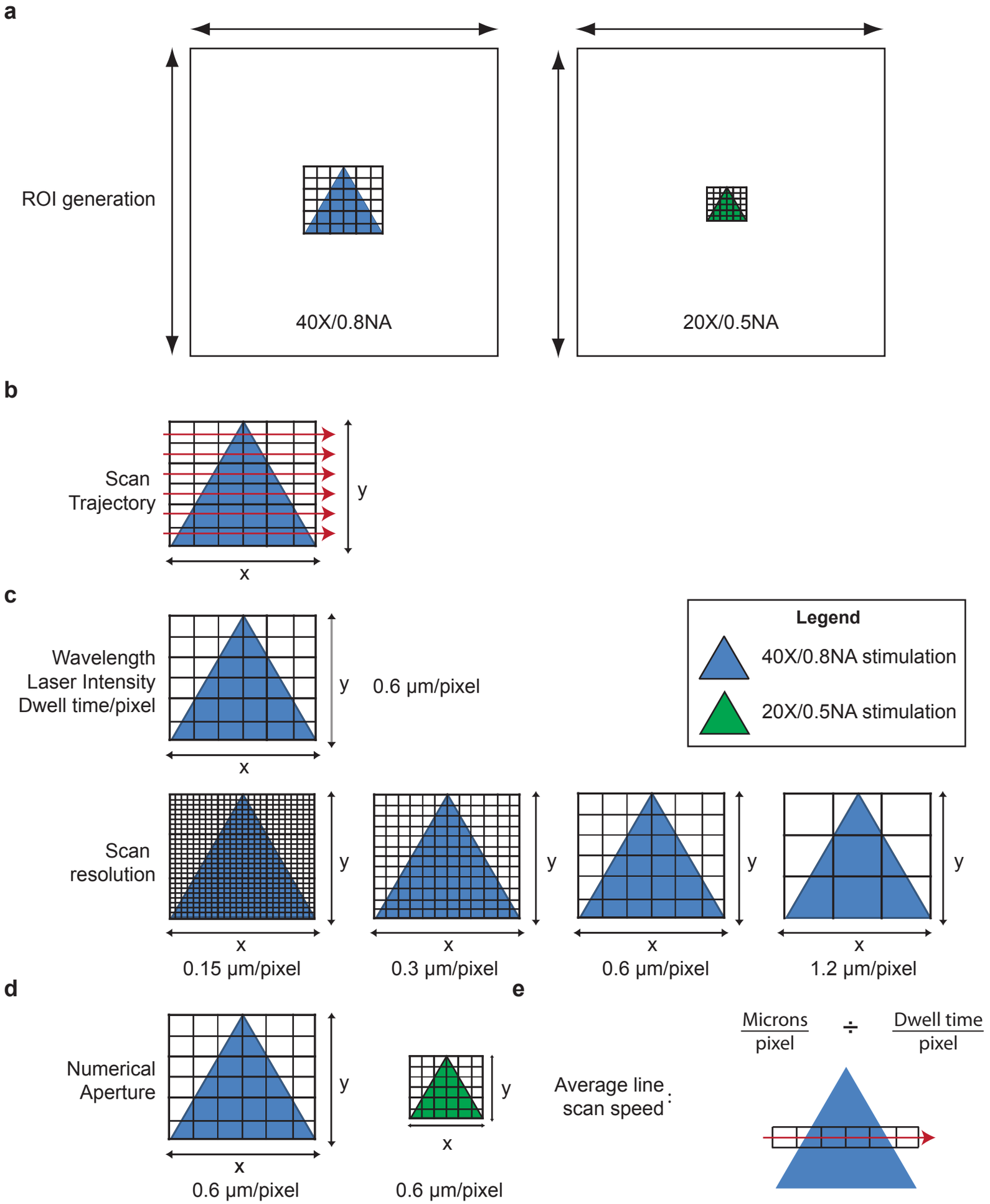

Nature Methods: doi:10.1038/nmeth.2215

Supplementary Figure 11. Schematics illustrating different two-photon LSM configurations and scan protocols relevant to raster-scanning two-photon optogenetics. a. Schematic of ROI generation for the 40× and 20× objective cases. Large boxes indicate the whole field of view (FOV) for the objectives. Scan resolution numbers noted in figure legends above (e.g. 1.20 μm/pixel, 0.6 μm/pixel, 0.3 μm/pixel, and 0.15 μm/pixel) correspond to microns/pixel along the 'x' or 'y' directions. ROIs are typically generated at this zoom level and are selected around the perimeter of the cell. For culture preparations, ROI sizes typically ranged from 15x15 μm to 20x20 μm and for slice and *in vivo* preparations, ROI sizes were typically 10x10μm to 15x15 μm. **b.** Schematic of the typical raster scanning laser stimulation trajectory. Scans were made in a unidirectional manner going from left to right and then line to line. The red arrow indicates the direction of travel through each line of the ROI. **c.** Schematic at top indicates that pixels in the X and Y directions used to illuminate a given cell (shown as the grid superimposed on the cell) are not varied during testing across wavelength, laser intensity, and dwell time/pixel. 0.6 μm/pixel is the scan resolution in this illustrated baseline case. Diagrams at bottom show variation in the scan resolution used to illuminate each cell (represented as the grid superimposed on the cell) in the X and Y directions while testing across different scan resolutions: 1.20 μm/pixel, 0.6 μm/pixel, 0.3 μm/pixel, and 0.15 μm/pixel, keeping dwell time, wavelength, and laser intensity constant. **d.** Schematic of the scan resolution in the X and Y directions while testing across two different numerical aperture objectives. 0.6 μm/pixel is the scan resolution in the 40×/0.8NA case and in the 20×/0.5NA case. In each case, scan speed is equivalent. **e.** Mean line scan speed is the scan resolution (microns/pixel divided by the dwell time/pixel. Red arrow indicates the direction of two-photon laser raster scanning for this line.

wavelength (nm)	pulse width (fs)
800	242
820	238
840	238
860	238
880	237
900	237
920	236
940	237
960	233
980	231
1000	232
1020	230
1040	229

Supplementary Table 1. Pulse width properties across wavelength for Coherent Ultra II Ti-Sapphire Laser. Pulse width measurements taken at the back-aperture of the objective with the two-photon illumination setup described in the methods. Note that pulse widths across all wavelengths were typically within 6% of each other.

Single cell manipulation goal	Reccommended 2P-suitable opsins	Excitation maximum (nm)	Suggested objective
Driving spikes with light separated from 800-1030nm band	$C1V1_T$	1040 or longer	20×/0.5NA
Bi-stable modulation	$ChR2_{AR}$	940	40×/0.8NA
Spike inhibition	eArch3.0	1040 or longer	20×/0.5NA

Supplementary Table 2. Two-photon optogenetic tool summary. Summary chart displaying suitable opsins for single-cell two-photon optogenetic spike generation, bistable modulation, and spike inhibition. Although the novel shorter wavelength-driven engineered opsins also generate two-photon-elicited responses at least as robust as those elicited by the C1V1 family, as shown here (especially the TC variants; **Supplementary Fig. 4d** vs. **Fig. 1f**) and are likely to be useful for 2P optogenetic applications in their own right, it is also likely that driving spikes with light separated from the 800-1030 nm spectral band (as with the C1V1 family) will be particularly useful for integration with the broad range of labels and indicators that are robustly sensitive in this range but which display virtually no responsivity at 1040 nm or longer (including GCaMPs and other GFP-based tools, OGB-1, and the like).